

# Atmospheric Sounding at JPL: Current and Future Technologies

Steven E. Broberg\*<sup>a</sup>, Thomas S. Pagano<sup>a</sup>, Hartmut H. Aumann<sup>a</sup>, Larrabee Strow<sup>b</sup>, Steven L. Gaiser<sup>a</sup>

<sup>a</sup>Jet Propulsion Laboratory, California Institute of Technology, Pasadena, CA 91109

<sup>b</sup>University of Maryland Baltimore County, Baltimore, MD

## ABSTRACT

JPL is currently managing the instrument operations, calibration and data system for the Atmospheric Infrared Sounder (AIRS) on the EOS Aqua spacecraft. Aqua was launched on May 4, 2002 from Vandenberg Air Force Base. AIRS has 2378 infrared channels with high spectral resolution (1200) covering the 3.7 to 15.4 micron wavelength range. AIRS data is used to produce temperature and humidity profiles useful in predicting weather and monitoring long term climate. We discuss lessons learned on AIRS in the development and operations as well as plans for next generation systems including SIRAS, a wide field hyperspectral infrared imaging spectrometer which offers AIRS spectral performance at 24x the spatial resolution.

Keywords: Hyperspectral, infrared, atmospheric, sounding

## 1. INTRODUCTION

The Atmospheric Infrared Sounder (AIRS) shown in Figure 1 is the first hyperspectral infrared sounder developed by the National Aeronautics and Space Administration (NASA) in support of operational weather forecasting by the National Oceanic and Atmospheric Administration (NOAA). The AIRS instrument represents the culmination of years of technology development in the area of infrared spaceborne instrumentation. Technology development in the areas of optical design, filter and optical coatings, electronic instrumentation, cryogenic cooling, and detector materials and readouts were all necessary in order to develop the system that flies today.

The AIRS instrument incorporates numerous advances in infrared sensing technology to achieve a high level of measurement sensitivity, precision, and accuracy. This includes a temperature controlled grating and long wavelength cutoff HgCdTe infrared detectors actively cooled to 58K by a pulse tube cryocooler.

The next generation of atmospheric infrared sounding instruments will require higher spatial resolution, possibly higher spectral resolution, better sensitivity, and smaller packaging. Achieving a significant improvement in any one of these areas would be a major advancement. NASA has chosen to emphasize two areas in recent technology development activities under the Instrument Incubator Program (IIP) with its sponsorship of the Spaceborne Infrared Atmospheric Sounder (SIRAS), an instrument concept which offers performance comparable to that of AIRS in a smaller package with higher spatial resolution.



Figure 1. The Atmospheric Infrared Sounder (AIRS).

\*Correspondance: E-Mail: [sbroberg@jpl.nasa.gov](mailto:sbroberg@jpl.nasa.gov); Telephone: +1 818 354-1554; Fax: +1 818 393-4918

This paper briefly reviews the AIRS measurement requirements and instrument description<sup>1</sup>, discusses pre-flight/in-flight spectrometer performance and lessons learned from operational experience<sup>1,2,3</sup>, and lastly presents the SIRAS concept's current implementation<sup>4</sup> and future development plans and opportunities.

## 2. AIRS MEASUREMENT REQUIREMENTS AND INSTRUMENT SPECIFICATIONS

Requirements for atmospheric sounding were first established in the late 50's<sup>5</sup>. The NOAA polar orbiting satellite systems have supported operational weather forecasting with HIRS (High Resolution Infrared Sounder) and the Microwave Sounding Unit (MSU) derived global temperature and moisture soundings since the late 70's. After analyzing the impact of the first ten years of HIRS/MSU data on weather forecast accuracy, the World Meteorological Organization (WMO) in 1987 determined that global temperature and moisture soundings with radiosonde accuracy are required to significantly improve the weather forecast<sup>6</sup>. Radiosonde accuracy is equivalent to profiles with 1 K rms accuracy in 1 km thick layers and humidity profiles with a 10% accuracy in the troposphere. An extensive effort of data simulation and retrieval algorithm development was required to establish instrument measurement requirements in the areas of spectral coverage, resolution, calibration, stability, and spatial response characteristics including alignment, uniformity, and measurement simultaneity, radiometric and photometric calibration and sensitivity to meet the WMO requirements. The 1 K / 1 km requirements can only be met by increasing the spectral resolution of the infrared sounder by about one order of magnitude, from the  $\lambda/\Delta\lambda=100$  resolving power of HIRS-2 to the hyperspectral  $\lambda/\Delta\lambda=1200$  resolving power of AIRS. Sensitivity requirements, expressed as Noise Equivalent Differential Temperature, NE $\Delta$ T, referred to a 250 K target temperature, range from 0.14 K in the critical 4.2 $\mu$ m lower tropospheric sounding wavelengths to 0.35 K in the 15  $\mu$ m upper tropospheric sounding region. These requirements are captured in The AIRS Functional Requirements Document (FRD)<sup>7</sup> which governed the design and development of the instrument.

AIRS, with spectral coverage from 3.7 to 15.4  $\mu$ m, working together with the Advanced Microwave Sounding Unit (AMSU, 27-89 GHz) and the Microwave Humidity Sounder (HSB, 150 – 187GHz), form a complementary sounding system for NASA's Earth Observing System (EOS), designed by NASA to support the operational weather forecasting effort of NOAA.

## 3. AIRS INSTRUMENT DESCRIPTION

The AIRS instrument provides spectral coverage in the 3.74-4.61  $\mu$ m, 6.20-8.22  $\mu$ m, and 8.8-15.4  $\mu$ m infrared wavebands at a nominal spectral resolution  $\lambda/\Delta\lambda = 1200$ , with 2378 spectral samples. A cross section of the scan head assembly is shown in Figure 2. A 360 degree rotation of the scan mirror generates a scan line of IR data every 2.667 seconds. The scan mirror motor has two speeds: During the first 2 seconds it rotates at 49.5 degrees/second, generating a scan line with 90 footprints of the earth scene, each with a 1.1 degree diameter IFOV. During the remaining 0.667 seconds the scan mirror completes one revolution with four independent views of cold space, one view into a 310 K radiometric calibrator called the On-Board Calibrator (OBC) Blackbody, one view into a spectral reference source (Parylene), and one view into a photometric calibrator. The VIS/NIR photometer, which contains four spectral bands, each with nine pixels along track, with a 0.185 degree IFOV, is boresighted to the IR spectrometer to allow simultaneous visible and infrared scene measurements.

The diffraction grating in the IR spectrometer disperses the radiation onto 17 linear arrays of HgCdTe detectors (see Figure 3) in grating orders 3 through 11. Each linear array is comprised of N elements (where N ranges from 94 to 192) by two rows (A and B) for redundancy. Gain tables in the electronics determine whether each channel uses the A-side or B-side detector or both. The IR spectrometer is cooled to 150 K by a two stage radiative cooler. The IR

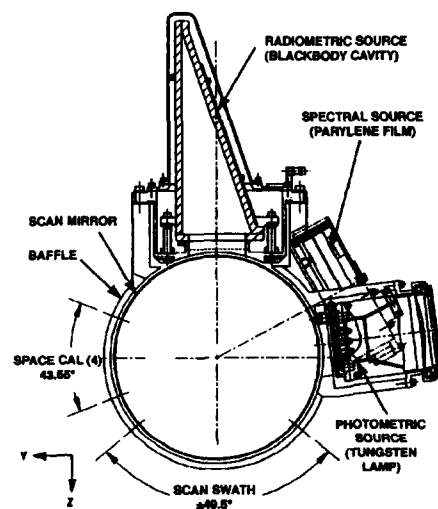


Figure 2. AIRS Scan Assembly.

focal plane is cooled to 60 K by a Stirling/pulse tube cryocooler. The scan mirror is cooled to about 265 K by radiative coupling to the Earth and space and to the 150 K IR spectrometer. Cooling of the IR optics and detectors is necessary to achieve the required instrument sensitivity. The VIS/NIR photometer uses optical filters to define four spectral bands in the 400 nm to 1000 nm region. The VIS/NIR detectors are not cooled and operate in the 293 K to 300 K ambient range of the instrument housing.

Signals from both the IR spectrometer and the VIS/NIR photometer are passed through onboard signal and data processing electronics, which perform functions of radiation circumvention, gain weighting and offset subtraction, signal integration, and output formatting and buffering to the high rate science data bus. In addition, the AIRS instrument contains command and control electronics whose functions include communications with the satellite platform, instrument redundancy reconfiguration, the generation of timing and control signals necessary for instrument operation, and collection of instrument engineering and housekeeping data.

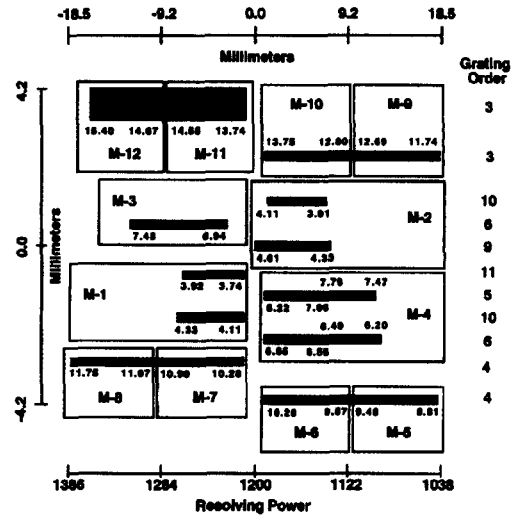


Figure 3. AIRS FPA Layout.

The Stirling/pulse tube cryocoolers are driven by separate electronics which control the phase and amplitude of the compressor moving elements to minimize vibration and to accurately control the temperature. Heat from the electronics is removed through coldplates connected to the spacecraft's heat rejection system.

#### 4. AIRS PERFORMANCE MEASUREMENT RESULTS

Careful pre-flight and in-flight characterization of the AIRS instrument performance is necessary to provide quantitative information on the random and systematic errors that result during the in-flight measurement program. A comprehensive test program was developed to address all areas of the calibration and to characterize the radiometric, spatial and spectral performance of the instrument. In the following sections we present the most recent understanding of the AIRS performance. The data are continually under evaluation and we will continue to remove any systematic errors as more information is obtained.

##### 4.1 Imagery Evaluation

Figure 4 shows a three level representation of the first light image from AIRS, taken near the coast of West Africa minutes after the AIRS IR spectrometer was activated. The image at the top of the figure shows a brightness temperature map for one of the 2378 infrared channels measured by AIRS. Expansion of a single pixel shows atmospheric features as expected. Further examination of the spectra highlights we see the CO<sub>2</sub> emission peak at 667 cm<sup>-1</sup>.

##### 4.2 Radiometric performance

The AIRS radiometric performance can be categorized into radiometric accuracy and sensitivity. The radiometric accuracy is dependent on the systematic errors that result from the pre-flight calibration. The on-board calibrator (OBC) blackbody is calibrated relative to an external NIST-traceable large area blackbody (LABB) using AIRS itself to make the transfer. Residual systematic errors for AIRS are less than 0.2K at 265K for all channels. Initial in-flight evaluation of radiometric accuracy has been verified to the 0.5K level<sup>8</sup>.

##### 4.2.1 Radiometric accuracy

##### 4.2.1.1 Pre-flight calibration residuals

The calibration equation, N (radiance) vs dn (data number) for AIRS is a second order polynomial modified by a small polarization correction term to account for the modulation of the scene radiance by coupling of the scan mirror and

## AIRS First Light Spectra

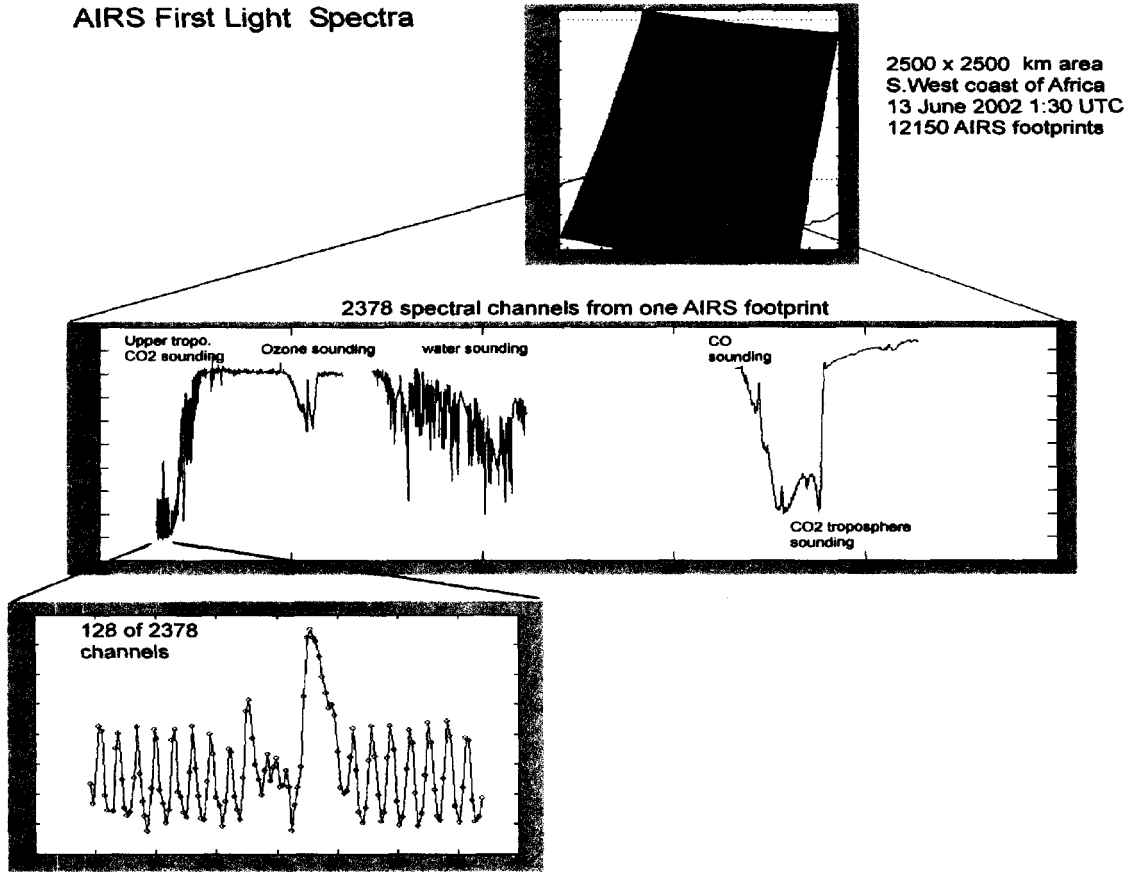


Figure 4. AIRS First Light data meets expectations.

spectrometer polarization as the scan mirror rotates:

$$N = \frac{a_0 + a_1(dn - dn_{sv}) + a_2(dn - dn_{sv})^2}{[1 + p_r p_t \cos(\theta - \delta)]}$$

Where  $p_r$   $p_t$  are the polarization factors for the scan mirror (r) and the spectrometer (t), and  $\theta$  and  $\delta$  are the angles of the scan mirror and spectrometer polarization orientation respectively. The offset term,  $a_0$  is due to the modulation of the emission of the scan mirror due to coupling of polarization with the spectrometer and varies with scan angle

$$a_0(\theta) = N_{sm} p_r p_t [\cos 2(\theta - \delta) \cdot \cos 2\delta]$$

The first order term  $a_1$  is the instrument gain and is calculated in-orbit using the  $dn$ 's from the OBC blackbody and space and the OBC radiance and solving the above calibration equation for  $a_1$  at the angles of the OBC of 180 degrees.

$$a_1 = \frac{\epsilon N_{obc}(1 + p_r p_t \cos 2\delta) - a_0(\theta_{obc}) - a_2(dn_{obc} - dn_{sv})^2}{(dn_{obc} - dn_{sv})}$$

When we acquire the stepped linearity data using the LABB, we simultaneously acquire data from the OBC Blackbody. The gain correction term,  $\epsilon$ , is the ratio of the radiance computed using the ground calibration coefficients to the radiance

computed from the known LABB temperature (as derived from the temperature sensors). The correction term is on the order of  $\pm 0.3\%$  as shown in Figure 5. This variance is most likely due to spatial response differences amongst the various modules in the near field.

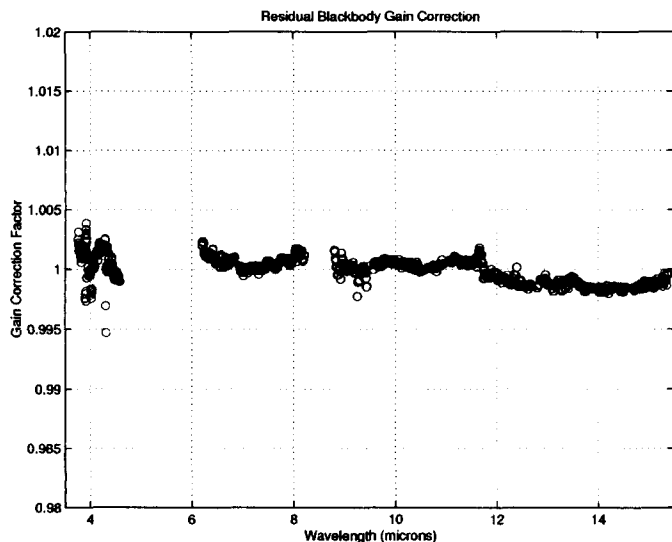
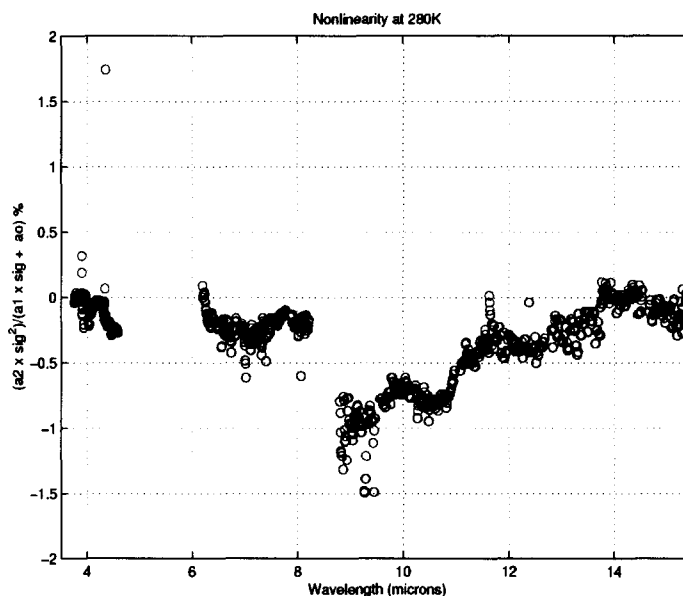


Figure 5. (left). AIRS Gain Correction. The correction is the ratio of emission from the OBC and LABB. We see less than  $\pm 0.25\%$  correction for most channels.

The nonlinearity of the AIRS is shown in Figure 6. We see most channels are linear to better than 0.5% with a few in the 9-11  $\mu\text{m}$  region up to 1.5%. This excellent linearity makes the calibration errors less dependent on knowledge of the second order term in orbit and improves the overall calibration.

Figure 6 (right). AIRS Nonlinearity. Nonlinearity is calculated as the ratio of the 2<sup>nd</sup> order contribution to the derived radiance to the sum of the 1<sup>st</sup> and 2<sup>nd</sup> terms. We see better than 0.5% nonlinearity for most channels, except in the 9-11  $\mu\text{m}$  region where we are less than 1.5%. This low nonlinearity will facilitate radiometric calibration in orbit.



The final test of the radiometric calibration was to apply the calibration algorithm to test data obtained during T/V testing. We calculate  $a_0$  from the polarization equation expected for radiometric offset as was discussed earlier.  $a_1$  is calculated using the gain correction term and OBC signals and temperatures, and  $a_2$  is obtained from the stepped linearity test. The residual error is defined as the difference in radiance between the derived radiance and the expected radiance for a unity emissivity blackbody at the temperature of the LABB, expressed as a temperature difference at the observed

temperature. Figure 7 shows residuals of less than 0.1-0.2 K at 250 K indicating we have an excellent calibration. We attribute this excellent performance to the cooled and actively controlled spectrometer temperature and the high system linearity.

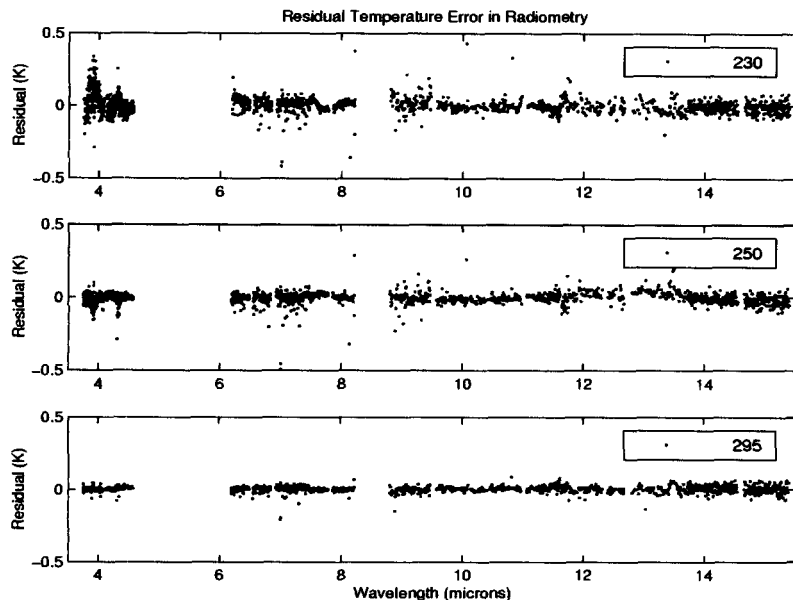


Figure 7. (left). Residual Calibration Uncertainty. The residual calibration error was calculated by applying the calibration coefficients,  $a_0$ ,  $a_1$  (calculated using the OBC), and  $a_2$  as would be done during on-orbit operations to data acquired at three different temperatures during thermal vacuum testing. We see better than 0.1-0.2 K calibration residuals at 250K.

#### 4.2.1.2 Polarization performance

Early on in the AIRS program, it was acknowledged that the polarization of AIRS grating spectrometer couples with the scan mirror polarization to produce a scan angle dependent radiometric modulation. This modulation is small, but not negligible and accurate quantification of the system polarization is necessary to correct the radiometry. Reference 9 discusses the conditions of the test and data acquisition of the polarization data. Reference 10 discusses how these data are used to correct for the scan angle dependent radiometry.

#### 4.2.2 Radiometric sensitivity

Figure 8 shows the measured RMS noise for AIRS expressed as NEdT at 250 K. The figure compares the pre-flight noise to that determined in-orbit using identical techniques. We see good agreement between the pre-flight and in-orbit measurements, indicating the instrument is operating as expected. We also see fewer outliers in the flight data. This is a consequence of an improved process for optimizing the gain tables that select the combination of A-side and B-side detectors to use in a given channel. The process for selecting which or both of the A-side or B-side detectors is used for any given channel involves careful characterization and evaluation of the noise and gain properties of each detector. The standard deviation ( $\sigma$ ) of the noise data acquired while viewing space is first calculated and called the NEdn. We first

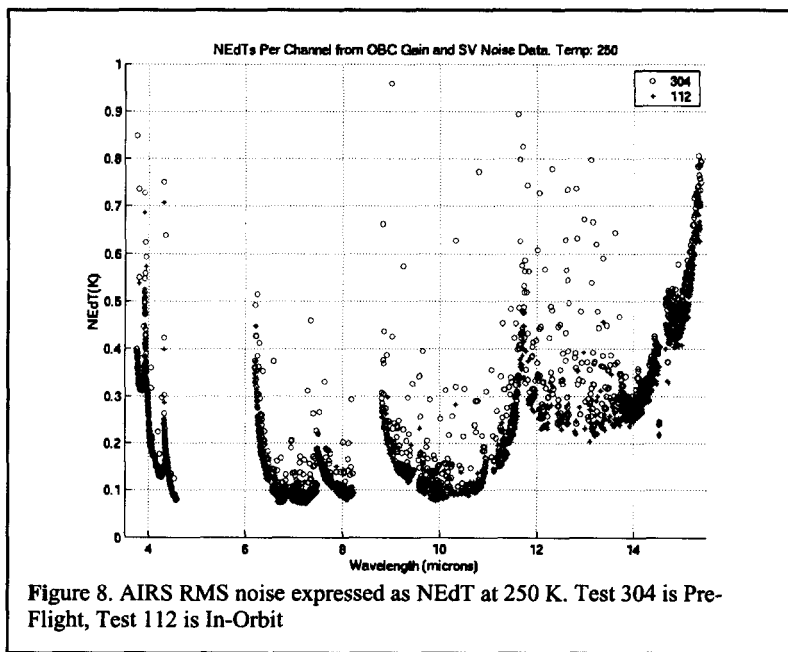


Figure 8. AIRS RMS noise expressed as NEdT at 250 K. Test 304 is Pre-Flight, Test 112 is In-Orbit

look at the magnitude of the NEDn; any detector with NEDn greater than 3 times the quadratic fit to the NEDn for the array is called noncompliant.

### 4.3 Spectral performance

The AIRS-Radiative Transfer Algorithm (AIRS-RTA) needs extremely accurate spectral response functions (SRF) for each AIRS channel to ensure that the AIRS-RTA calculated radiances are within the AIRS noise level. Since AIRS retrieves atmospheric temperature and humidity profiles by comparing observed and computed radiances, the final accuracy of the AIRS products is intimately dependent on well-known SRFs.

The relevant parameters needed to characterize the SRFs are spectral centroid, width, and shape. The centroids must be known to 1% of the SRF width, the widths to 1-3% (of a width), and the shape to  $\approx 0.1\%$  in the wings. In practice these requirements can be relaxed significantly for channels that do not cover sharp features in the atmospheric spectrum. The determination of the shape of each SRF was a pre-flight activity<sup>1</sup>. Spectral centroids are determined by correlating observed radiance spectra with pre-calculated modeled radiances. AIRS in-orbit spectral calibration consists of the determination of the centroids of the Spectral Response Functions (SRFs) for each channel.

#### 4.3.1.1 Pre-flight spectral calibration methodology

The AIRS spectral calibration methodology utilized a very unique design where the output of a high spectral resolution Michelson interferometer was fed into AIRS. The AIRS clock controlled the stepping of the interferometer (a Bruker), allowing AIRS to integrate the signal over 1 to n effective fields-of-view for each step of the interferometer. The final spectral calibration data was acquired with  $n = 6$ . The Bruker was run in double-sided mode, with a maximum optical path difference of 2.88 cm.

Each AIRS detector produced an interferogram, whose Fourier transform is the spectral response function (SRF) for that detector. Each interferogram is phase-corrected. Absolute wavenumber calibration was achieved by placing a gas cell containing low-pressure carbon monoxide between the interferometer and AIRS, which superimposed several carbon-monoxide absorption lines on several SRFs in the  $2100\text{ cm}^{-1}$  spectral region. The interferogram data is zero-filled to 10 cm before taking the Fourier transform.

The AIRS order sorting entrance slit filters are not wedged, introducing interference fringes into the SRFs with a magnitude of  $\approx 2\text{-}8\%$  peak-to-peak and a period of  $\approx 1.2\text{ cm}^{-1}$ . Since the SRF centroids may shift during launch, and because the SRF centroids vary with temperature differently than the phase of these fringes, we need to characterize the SRFs and fringes separately. This is easily accomplished since the Bruker SRF data is much higher resolution than the fringes. The detailed procedures are too complicated to completely describe here, but the end result is that we can accurately remove the fringe effects from the SRF for the purpose of deriving the AIRS grating model centroids and grating spectrometer SRF shape. We have also characterized the shape of the fringes and their dependence on temperature. The final SRF used in-orbit will be the "pure" grating SRF multiplied by the fringes, once their phase is known in orbit. (We can compute the fringe phase from the entrance filter temperature.) The following discussion on the SRFs and grating model refers to the "de-fringed" SRFs.

The variation of the SRF centroids between different tests, and between the A and B-side detectors is within our specification (1% of a width), although we can detect A to B-side shifts. In orbit we will generally use an almost equal

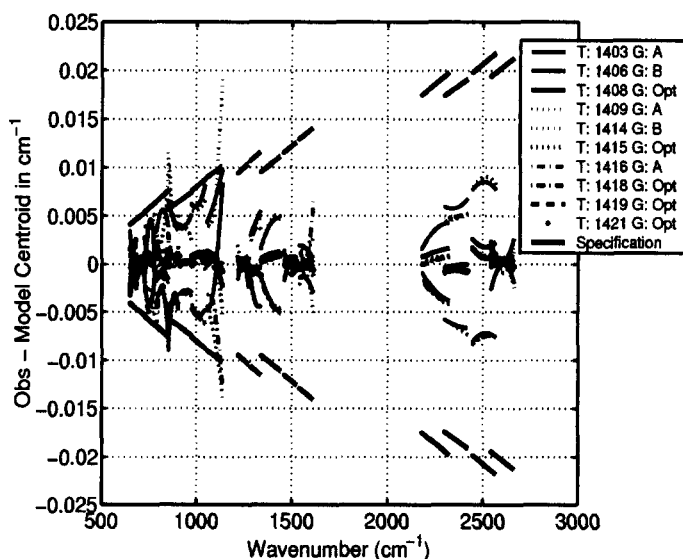


Figure 9: Deviation of centroids from test mean, T = 161K

combination of A and B-side signals (called “Opt” for optimum) for the channel radiance, so averaging all A and B-side tests together for the grating model will be sufficiently accurate. Figure 9 shows the deviations of the grating model fits from the mean of all tests for the  $T = 161$  K calibration tests. This figure highlights the sensitivity of the spectral calibration test setup and the high signal-to-noise of these measurements. The array position are found to vary slightly with temperature by an amount equivalent to a centroid shift of 2.2% of a width per K. The effective focal lengths  $F_k$ , do not exhibit any dependence on temperature.

#### 4.3.1.2 Pre-flight SRF width and shape determination

The SRF width measurements showed no variation with temperature, and are determined to the required specs (1-3%) or better. The observed widths are found to be 3-14% narrower than expected, which is a curious result given that the SRF widths are almost totally determined by the combination of the grating dispersion and the entrance slit widths. Figure 10 shows measured SRFs averaged over three broad wavenumber ranges. These are averages of channels over several arrays, nominally ~5-6 arrays per average. The SRFs are nominally 100 microns wide, so this figure shows that the SRF magnitude is below 0.1% of its peak value at 3 full widths from the channel center.

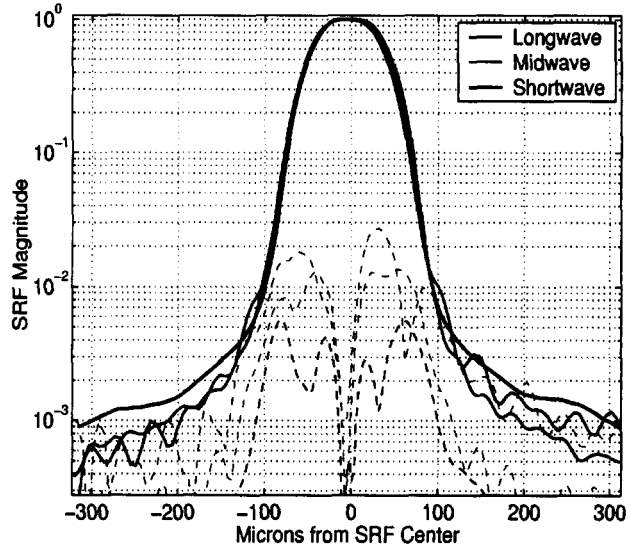


Figure 10: Observed SRFs averaged for three broad wavenumber regions. The dashed lines are the standard deviation of these averages.

The observed SRFs are fit to a simple analytic function (roughly the sum of a Lorentz plus a Gaussian shape) with good results. Our main goal for these fits is to smooth noise in the SRF wing. These fits included the effects of the Bruker, which introduces very noticeable sinc ringing in the longest wave arrays. Variations of the SRFs within a single array is undetectable and below our specifications, allowing us to use a single shape (but not width) for each channel in each array. Variations in the SRF shape among arrays is also quite small, but big enough that we need to take them into account.

All results presented were acquired after insertion of a field mask at the field stop of the telescope, narrowing the AIRS IFOV to 0.6 degrees in the cross-track direction. This field mask was inserted to reduce field dependent spectral sensitivity, but cost the system 35% in signal. The tradeoff worked and we now have the spectral uniformity across the field as desired.

#### 4.3.2 In-flight spectral centroid determination

Spectral centroids of the SRFs are determined in orbit by correlating observed upwelling radiance spectra with pre-calculated, modeled radiance spectra. Because some parts of the spectrum are more suitable than others, this is done for many separate spectral regions (referred to as 'spectral features'), rather than for the focal plane as a whole. The resultant correlations are fit to, and the location

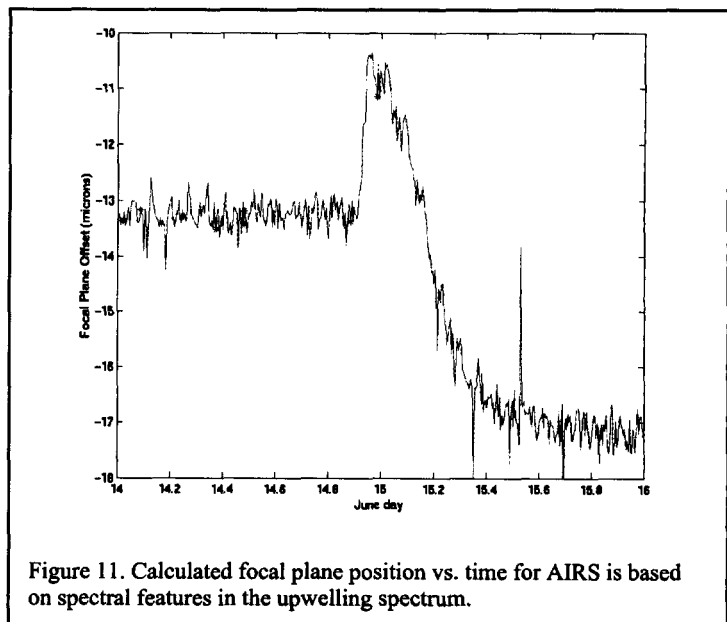


Figure 11. Calculated focal plane position vs. time for AIRS is based on spectral features in the upwelling spectrum.

of the maximum correlation is determined. The focal plane shift corresponding to the maximum correlation is the observed shift of the feature. By combining the observed shifts from several different spectral features, the focal plane shift is determined. From that shift, the centroids of each detector can be calculated. Figure 11 shows calculated focal plane position as a function of time. One micron of focal plane shift corresponds to centroid frequency shifts of one percent of each channel's full width at half maximum. Late on June 14, the spectrometer temperature was lowered, causing the observed change in calculated focal plane offset. During stable periods, the standard deviation of individual calculations of focal plane offset is 0.25 microns. Averaging these values over the thermal time constant of the instrument (twelve hours) reduces the uncertainty in the mean shift to less than 0.02 microns relative. Absolute accuracy of better than 0.5 microns, corresponding to one half of one percent of  $\Delta v$ , is indicated by analysis of in-orbit channel phase test results and by preliminary analysis of modeled upwelling radiance spectra.

#### 4.4 Spatial response

##### 4.4.1 Near Field Response

The AIRS spatial response was measured during pre-flight testing using the Spatial Collimator Source (SCS). In this experiment, a  $0.1^\circ$  circular spot was scanned in two dimensions across the  $1.1^\circ$  field of view of the AIRS. The AIRS response was measured for all of the 2378 channels. Examples of these response profiles are shown in Figure 14 (left). Each contour line is about 20% of full scale. The profiles shown here were obtained prior to insertion of the field mask mentioned previously, and do not include the scanning motion of the instrument. The scanning motion tends to greatly homogenize the spatial response along the scanning direction. Limited data sets were obtained to verify that a simulation of the resulting spatial response with the field mask in place were valid. We then used the simulation software to compute the co-registration of the AIRS reference channels (3 channels near center and two ends of each of the 17 modules). A figure of merit of the coregistration is the  $C_{ij}$ , where

$$C_{ij} = 1 - (\iint |s_i - s_j| dx dy) / (\iint s_i dx dy + \iint s_j dx dy),$$

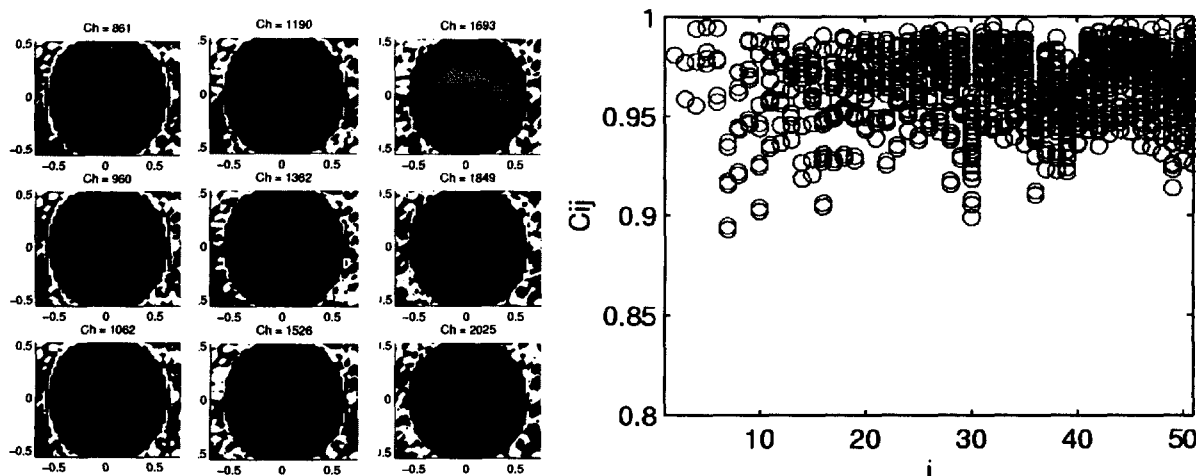


Figure 12 (left). Static Scan Spatial Response of AIRS Channels. (right). Simulated  $C_{ij}$ , scanning with field mask

where  $s_k = s_k(x,y)$  is the two dimensional spatial response function of the  $k^{\text{th}}$  IR spectral channel, including the cross-track scan motion. Figure 12 (right) shows the  $C_{ij}$  for the 51 reference detectors. The  $C_{ij}$  does not meet the original requirements set forth in the FRD<sup>5</sup> for many channels, however, algorithmic techniques will be implemented in the science data processing software to mitigate the noncompliance.

## 5. OPERATIONAL EXPERIENCE

### 5.1 Icing of optics and cooler

The buildup of ice on the optics and cooler has had directly observable impact on the system transmission and the cooler drive percentage. Figure 13 illustrates the decrease in system transmission seen in each of AIRS 17 focal plane modules. The accumulation of ice on the optics stopped in September of '02. Figure 14 illustrates the increase in cooler drive percentage seen while operating with one cooler (with one redundant), and with two coolers operating concurrently. The switch to two cooler operations has resulted in a decrease in the rate of increase in the drive percentage, allowing for continued operations without a defrost cycle for possibly up to two years.

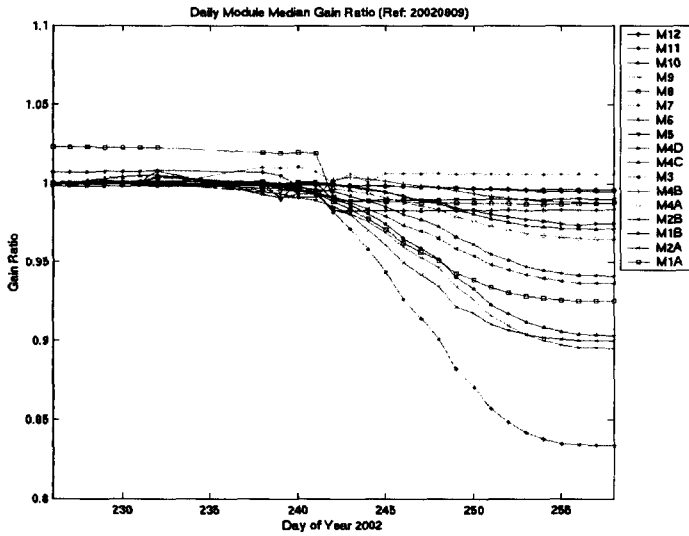


Figure 13. Ice impact on AIRS system transmission

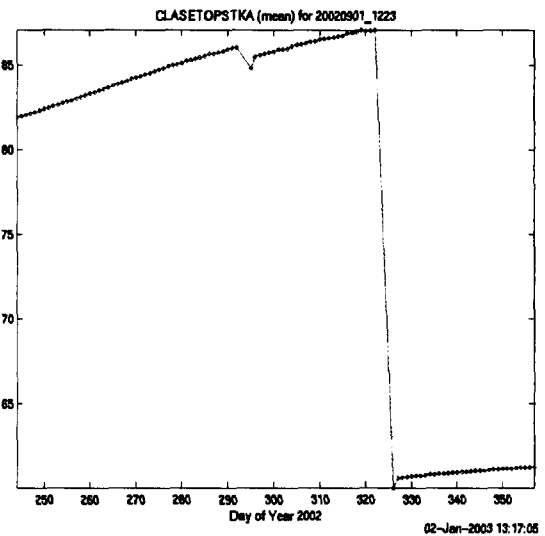


Figure 14. Cooler drive % increase with ice buildup, 1 & 2 coolers

### 5.2 Radiation circumvention

The AIRS instrument includes on-board signal processing to detect and remove signal spikes resulting from orbital proton radiation hits in the PV HgCdTe detector channels. The signals are internally sampled at 8 or 16 times the output signal rate, depending on the detector group. The radiation-hits affect only a single sample, resulting in significant isolated spikes, especially for the shorter wavelength detectors. The second difference of the signals is compared with a threshold value, programmable for each detector. For each threshold crossing, the processor substitutes for the signal sample in the output stream at that time with the mean of the samples in the input stream that occurred just before and after the detected hit. Thus, radiation-hit events are circumvented from the output stream, with nearly negligible effect on the radiometric accuracy of the signal after summing by 8 or 16 samples into the final output data stream. Figure 15 shows a time sequence of output signals (after the summation by 8 samples) for a selected detector used to detect  $3.9 \mu\text{m}$  IR radiation. This sequence was taken while the instrument was passing through the intense proton radiation environment of the SAA. The large spikes in the

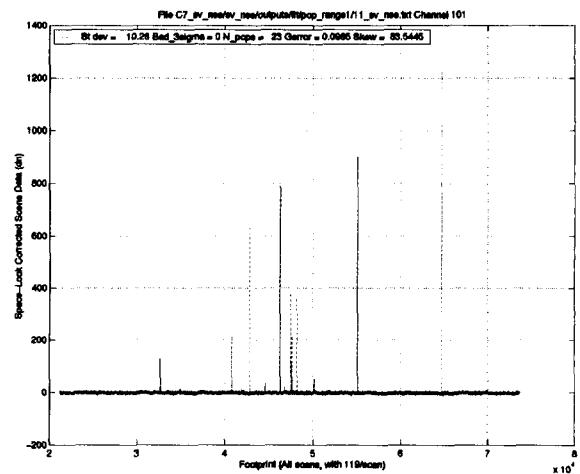


Figure 15. Time sequence of data shows radiation induced noise spikes

signal are the result of proton radiation hits in the detector.

The circumvention process involves acquiring data within and outside of the SAA, measuring the noise properties, and applying thresholds that satisfactorily remove the isolated noise spikes. This test was performed in orbit and thresholds of 5 times the RMS noise used for channels 0 to 1116 corresponding to the shortest wavelength modules.

Figure 16 shows the deviation from Gaussian behavior for all A side channels in AIRS measured in orbit. This term is calculated by comparing the histogram of data measured while viewing space to a pure Gaussian distribution and taking the deviation from ideal and normalizing to the integral. Data are shown for the normal operational mode in a low radiation part of the orbit (test 14), and with (test 34) and without (test 11) circumvention processing while inside the SAA. The process returns the noise histograms to their expected Gaussian shapes by eliminating the radiation hit spikes.

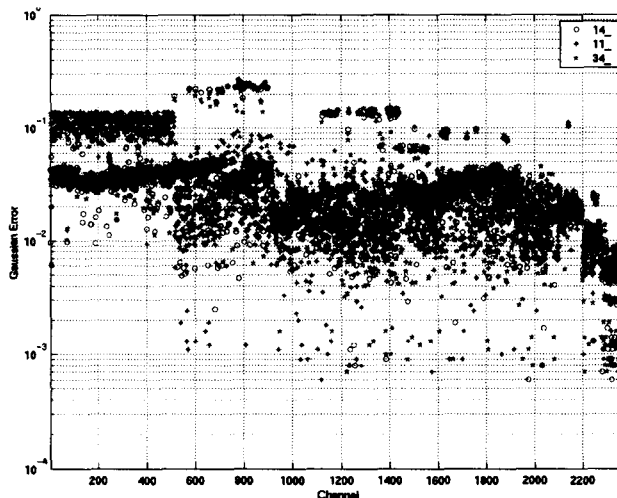


Figure 16. Deviation from Gaussian behavior for AIRS A-side detectors. Test 11 and 34 are in the SAA. Test 34 had radiation circumvention processing engaged.

We conclude that although radiation events can significantly degrade the noise performance of the shorter wavelength detectors, the radiation spike circumvention processing implemented in AIRS effectively eliminates the deleterious effects of radiation on detector sensitivity.

## 6. SIRAS - THE SPACEBORNE INFRARED ATMOSPHERIC SOUNDER

The AIRS represents the culmination of years of technology development in the area of infrared spaceborne instrumentation. Technology development in the areas of optical design, filter and optical coatings, electronic instrumentation, cryogenic cooling, and detector materials and readouts were all necessary in order to develop the system that flies today. Figure 17 shows some examples of major technology developments from the AIRS, SIRAS, and Integrated Multispectral Atmospheric Sounder (IMAS) programs including:

Motor Encoders, IR Calibration targets, and Dewars and Cryogenic Optics from BAE Systems on programs including: Motor Encoders, IR Calibration targets, and Dewars and Cryogenic Optics from BAE Systems on the AIRS

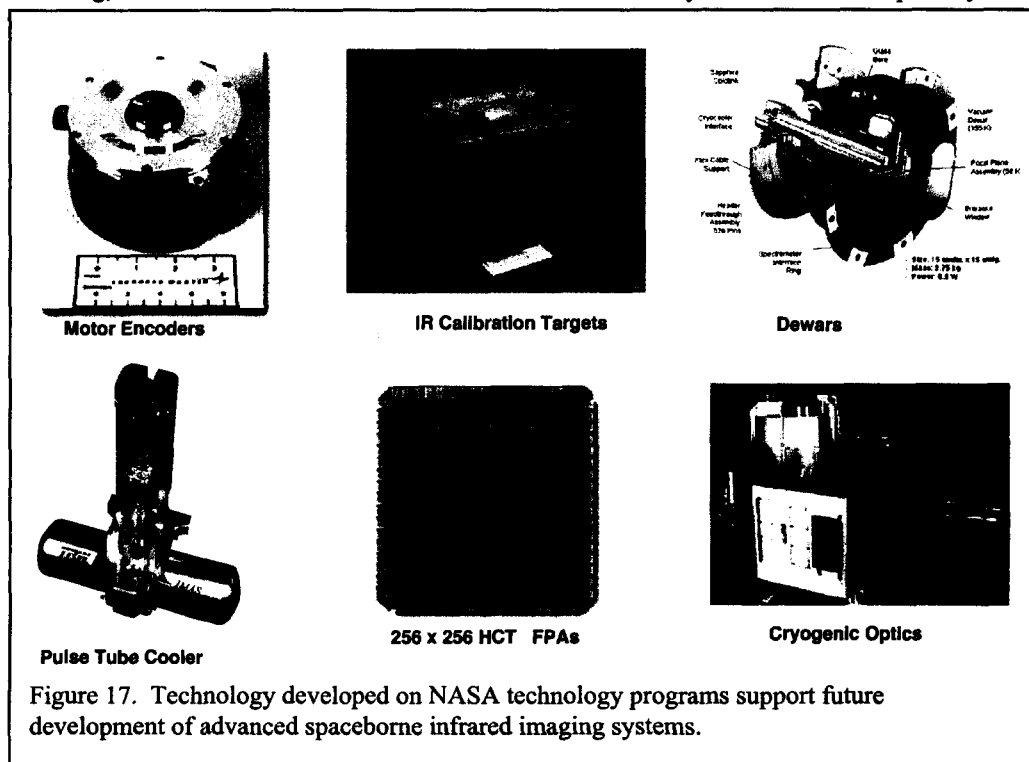


Figure 17. Technology developed on NASA technology programs support future development of advanced spaceborne infrared imaging systems.

project; the IMAS pulse tube cryogenic cooler built by TRW; and a 256 x 256 LWIR PV HgCdTe array under development on the SIRAS Instrument Incubator Program (IIP).

The next generation of atmospheric infrared sounding instruments will require higher spatial resolution, possibly higher spectral resolution, better sensitivity, and smaller packaging. Achieving a significant improvement in any one of these areas would be a major advancement. NASA has chosen to emphasize two areas in recent technology development activities under the Instrument Incubator Program (IIP).

The NASA Instrument Incubator Program has been established as a means to rapidly develop and demonstrate new technologies applicable to future Earth remote sensing science missions. The goal of IIP is to develop and demonstrate new technologies in a quick turn-around three-year program with the goal of having an instrument concept completed at this time that would be ready for space flight within three years.

The Spaceborne Infrared Atmospheric Sounder (SIRAS), shown in Figure 18, is an instrument concept for an infrared imaging spectrometer operating in the 3.7 to 15.4  $\mu\text{m}$  spectral region developed under NASA's Instrument Incubator Program (IIP). SIRAS was designed to meet the requirements of the Atmospheric Infrared Sounder (AIRS) instrument that is to be flown on the EOS-Aqua spacecraft, but in a smaller package and with higher spatial resolution. The AIRS has a  $\pm 49.5^\circ$  cross-track swath with 90 pixels at 13.5 km spatial resolution at nadir. The SIRAS provides 256 pixels cross-track at 0.56 km spatial resolution for a 145km swath. Cross-track and along-track pointing provides extended coverage. The improvement in spatial resolution can also facilitate use in higher Medium and Geosynchronous Earth Orbits.

The focus of the IIP hardware development undertaken in 1999-2000 was the design, fabrication, assembly, and test of an infrared spectrometer. This IR spectrometer takes advantage of wide field-of-view refractive optics and a high-dispersion grating and demonstrates the smallest possible solid state (no moving parts) IR spectrometer system that can be made at these wavelengths and at this resolution. The focus of this effort was to develop and demonstrate one of the four-spectrometer subsystems making up the SIRAS instrument. This was the longest wavelength spectrometer, that designed to operate in the 12 to 15.4 mm spectral region. This effort included developing all optical and mechanical hardware necessary in a flight-like configuration.

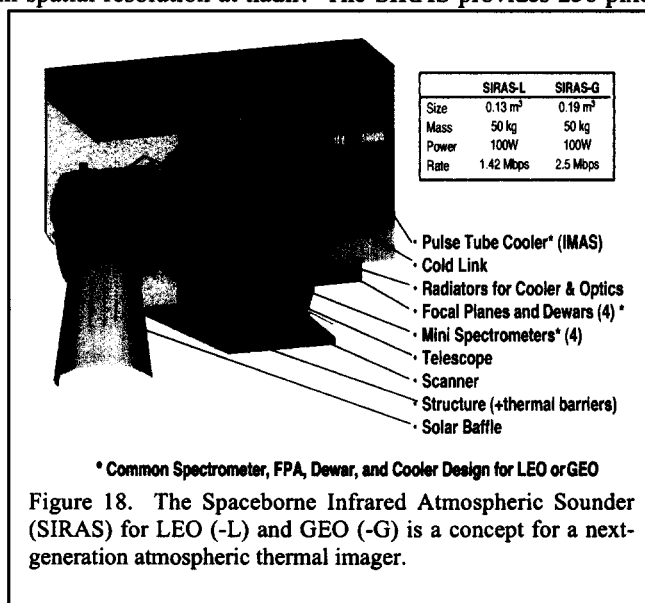


Figure 18. The Spaceborne Infrared Atmospheric Sounder (SIRAS) for LEO (-L) and GEO (-G) is a concept for a next-generation atmospheric thermal imager.

Figure 19 shows the spectrometer optical design, spectrometer hardware, spectrometer in the dewar and a spectra achieved. The development of the hardware included the use of exotic optical materials and designs, coatings for cryogenic temperatures, and opto-mechanical hardware implementation for a flight-like environment<sup>4</sup>. The instrument was cooled to 140K with the FPA cooled to 77K and testing was made through a window in the dewar. Measurements were taken of a laboratory lackbody in air at two different distances. The difference of the spectra were calculated and the resulting CO<sub>2</sub> spectra obtained. The results met the requirements of spectral resolution, coverage and fidelity set forth by the design all in very compact package. The spectrometer assembly shown in the figure weighs 2kg.

NASA recently awarded Ball Aerospace and Technologies Corporation (BATC) a contract to continue technology development of SIRAS in anticipation of its applicability to the GOES-R mission. JPL is investigation various mission scenarios to improve weather forecasting and data assimilation. Interest has been expressed for a SIRAS Aircraft exercise. The selection spectral region for the most recent award is the window channel, 8-12 microns. This is adequate for demonstrating the technology while offering an excellent tool for infrared land surface spectroscopy. Selection of

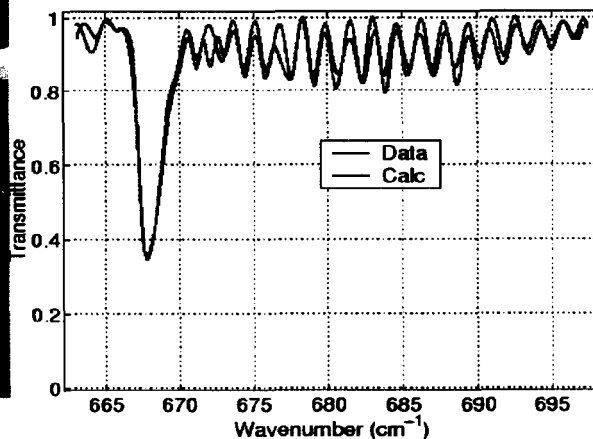
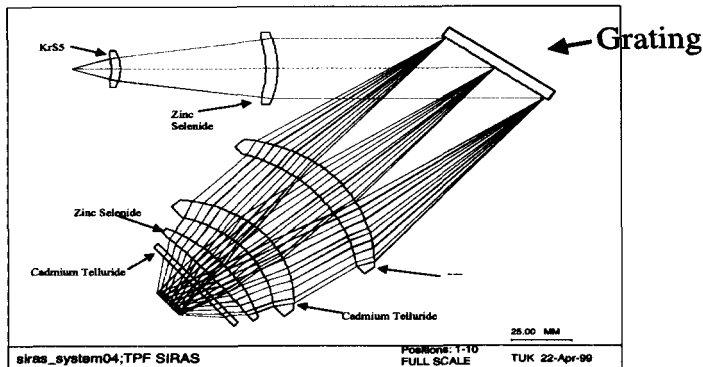


Figure 19 shows the spectrometer optical design, spectrometer hardware, spectrometer in the dewar and a spectra achieved.

proper spectral region allows for imaging of trace gasses such as  $\text{SO}_2$  or  $\text{CO}_2$ . Video camera versions of SIRAS are also being considered for special field applications.

## 7. SUMMARY

The AIRS instrument represents a major advance in passive IR remote sensing technology. We have observed 0.1-0.2K residual radiometric calibration uncertainty at 250K. We attribute this low uncertainty to the cooled and actively controlled spectrometer temperature and the high system linearity. Testing using a narrow source of 10% of the bandwidth has allowed us to meet our 1% of the bandwidth spectral calibration accuracy. The AIRS derived data about the atmosphere, land and oceans will be of unprecedented accuracy to support the operational weather prediction effort of NOAA and climate and global change research objectives of NASA. Investment in the SIRAS is providing the foundation for the next generation atmospheric sounder as well as providing opportunities for applications in spectroscopy and special field applications.

## ACKNOWLEDGMENTS

The AIRS instrument was designed, built and tested by BAE SYSTEMS, Lexington MA, under a systems contract with the Jet Propulsion Laboratory, Pasadena, CA. The calibration data analysis is the combined effort of the AIRS calibration team, including Steve Gaiser, Denise Hagan, and Ken Overoye and Margie Weiler of BAE SYSTEMS. The Jet Propulsion Laboratory, California Institute of Technology, operates under contract with the National Aeronautics and Space Administration.

## REFERENCES

1. T. Pagano et al., "Pre-launch Performance Characteristics of the Atmospheric Infrared Sounder (AIRS)", SPIE 4169-41, September 2000.
2. T. Pagano et al., "Early Calibration Results from the Atmospheric Infrared Sounder (AIRS)", SPIE 4891-09, October 2002.
3. T. Pagano, et. al, "On-Board Calibration Techniques and Test Results for the Atmospheric Infrared Sounder (AIRS)", SPIE 4814-38, July 2002.
4. T. Kampe, T. Pagano, J. Bergstrom, "SIRAS, The Spaceborne Infrared Atmospheric Sounder: an approach to next-generation infrared spectrometers for Earth remote sensing", SPIE 4485-12, August 2001.
5. L. D. Kaplan, "Inference of atmospheric structures from satellite remote radiation measurements", J. Opt. Soc. Am., Vol. 49, pp 1004-2007, 1959.
6. World Meteorological Organization, "The World Weather Watch Programme 1988-1997", WMO-No.691, 1987.
7. Jet Propulsion Laboratory, "AIRS Functional Requirements Document", JPL Internal Document D-8236, Rev.1., Oct.1992.
8. Aumann H. H. and T.S. Pagano, "Early Results from the Advanced Infrared Temperature Sounder (AIRS) on the EOS Aqua," Proc. SPIE Europto 23 September 2002, Crete, Greece
9. G. Gigioli and T. Pagano, "AIRS instrument polarization response: measurement methodology, SPIE 3759-30, July 1999
10. T. Pagano, et. al, "Scan Angle Dependent Radiometric Modulation due to Polarization for the Atmospheric Infrared Sounder (AIRS)", SPIE 4135-14, In Print August 2000.